

**PROCEEDINGS
TWELFTH WORKSHOP
GEOHERMAL RESERVOIR ENGINEERING**

January 20-22, 1987



**Henry J. Ramey, Jr., Paul Kruger, Frank G. Miller,
Roland N. Horne, William E. Brigham,
Jesus Rivera
Stanford Geothermal Program
Workshop Report SGP-TR-109***

DISCLAIMER

This report was prepared as an account of work sponsored by an agency of the United States Government. Neither the United States Government nor any agency Thereof, nor any of their employees, makes any warranty, express or implied, or assumes any legal liability or responsibility for the accuracy, completeness, or usefulness of any information, apparatus, product, or process disclosed, or represents that its use would not infringe privately owned rights. Reference herein to any specific commercial product, process, or service by trade name, trademark, manufacturer, or otherwise does not necessarily constitute or imply its endorsement, recommendation, or favoring by the United States Government or any agency thereof. The views and opinions of authors expressed herein do not necessarily state or reflect those of the United States Government or any agency thereof.

DISCLAIMER

Portions of this document may be illegible in electronic image products. Images are produced from the best available original document.

ON FLUID AND HEAT TRANSFER IN DEEP ZONES OF VAPOR-DOMINATED GEOTHERMAL RESERVOIRS

*K. Pruess**, *R. Celati†*, *C. Calore‡*, and *G. Cappetti†*

* Earth Sciences Division, Lawrence Berkeley Laboratory
University of California, Berkeley, California 94720

† Istituto Internazionale per le Ricerche Geotermiche,
CNR, Piazza Solferino 2, 56100 Pisa, Italy

‡ ENEL, Unita Nazionale Geotermica,
Via Andrea Pisano, 56100 Pisa, Italy

INTRODUCTION

The vapor-dominated reservoirs of Larderello, Italy, The Geysers, California, and Matsukawa, Japan, have been under exploitation for several decades. Much geological, geophysical, geochemical, and reservoir engineering information on these systems has been published in the technical literature. Conceptual models have been developed which explain important physical and chemical conditions and processes in these systems (Ferrara et al., 1970; Sestini, 1970; White et al. 1971; Truesdell and White, 1973; Weres et al., 1977; D'Amore and Truesdell, 1979; Pruess and Narasimhan, 1982).

Vapor-dominated reservoirs are overlain by a caprock of generally low permeability, in which heat transfer occurs mainly by conduction. In the main vapor-dominated zone vertical gradients of temperature and pressure are small, so that conductive heat flow is negligibly small. Heat transfer in these zones occurs by means of a vapor-liquid counterflow process known as "heat pipe" (White et al., 1971; Martin et al., 1976; Straus and Schubert, 1981; Pruess, 1985). Vapor originates at depth from boiling of liquid. It rises to shallower horizons where it condenses, depositing its large latent heat of vaporization. The condensate then returns to depth driven by gravity force.

Little is known about fluid and heat transfer processes, and thermodynamic conditions of formation fluids beneath the main permeable zones of vapor-dominated systems. Systematic long-term increases in production temperatures with strong superheating have been reported for Larderello (Sestini, 1970). These observations suggested that fluids with very high enthalpy can be delivered from greater depths (2-4 km). In recent years a programme of deep exploration has been carried out at Larderello by the Ente Nazionale per l'Energia Elettrica (ENEL), results of which have

been presented by Cappetti et al. (1985). Several wells have been drilled to depths of 3000 m and more, and temperatures in excess of 300 °C have been observed. More recently, similarly high temperatures and high-enthalpy fluids have been reported for a deep well at The Geysers (Drenick, 1986).

In this paper we present temperature data for deep horizons at Larderello, and we attempt to analyze the data with a view on identifying reservoir conditions and processes at depth. Of particular interest are the mechanisms and rates of fluid and heat flow in the natural state and in response to exploitation, and the permeability structure of the reservoir.

DATA ON DEEP TEMPERATURES

Temperature logs are run in Larderello wells during drilling stops mainly to locate permeable zones. In some cases drilling stops are sufficiently long to permit bottom-hole temperatures to stabilize at values indicative of formation conditions. For shorter drilling interruptions (24-48 hours) it is possible to estimate formation temperatures from a record of the temperature recovery at bottomhole (Barelli and Palama, 1981; Grant et al., 1982). Such estimation provides reliable results when formation permeability at bottomhole is low. After completion, temperatures tend to stabilize throughout the depth of the borehole, but the presence of internal flows [with heat loss and boiling and condensation effects] generally make wellbore temperatures different from formation temperatures. In some wells high rates of internal flow between different permeable intervals are present in shut-in conditions, so that in the vicinity of fluid entry points temperatures are relatively unperturbed by heat loss effects in the wellbore. However, due to the predominance of fracture permeability in Larderello it is generally not possible to correlate temperatures measured at a major

feed with formation temperatures at the same depth.

Because of these difficulties, only few reliable measurements of formation temperatures are available from Larderello. In Figure 1 we present temperature-depth data obtained from three productive wells located in the central area of Larderello, which has been under production for some forty years. Note that temperatures at any given depth are generally similar for the three wells. Down to approximately 500 m depth there is a conductive gradient of approximately 0.49 °C/m. From 500 to 2400 m depth there is a very small gradient of 0.015 °C/m, which is typical of the main zone of vapor-dominated systems. Substantially higher temperature gradients, approaching boiling point-for-depth (B.P.D.) conditions, are encountered at greater depth.

The temperatures of the fluids produced at Larderello have increased considerably over decades of exploitation (Sestini, 1970). It is not known how formation temperatures such as shown in Figure 1 differ from the conditions that were present before exploitation.

HEAT FLOW ANALYSIS

As an introduction into analyzing heat transfer conditions at depth we shall briefly discuss the natural state of a vapor-dominated system. The following observations and assumptions can be made:

- in the natural undisturbed state, heat transfer in vapor-dominated systems is essentially vertical; horizontal components of heat flux will only be significant at the reservoir margins, where temperature gradients have large horizontal components;
- in the natural state, a reservoir is close to steady-state conditions of fluid and heat flow; this together with the assumption made above implies that vertical heat flux is very nearly constant down to "great depth";
- total vertical heat flux contains conductive and convective components; convective heat transfer is accomplished by steam-water counterflow (heat pipe);
- in the natural state, steam-water counterflow will be very nearly balanced, so that net vertical fluid flux will be very small;
- the reservoir is in two-phase conditions all the way down to great depth where supercritical conditions may be reached (Cappetti et al., 1985).

On the basis of these assumptions it is possible to

write the total vertical heat flux as a sum of conductive and convective contributions (Martin et al., 1976). Assuming the z-axis to point downward, we have for upward heat flux:

$$Q = Q_{\text{conv}} + K \frac{dT}{dz} \quad (1)$$

$$Q_{\text{conv}} = k \frac{(\rho_l - \rho_v) h_{vl} g}{\frac{\mu_l}{k_{rl} \rho_l} + \frac{\mu_v}{k_{rv} \rho_v}} \quad (2)$$

$$\frac{dT}{dz} = \left(\frac{1}{\rho_v} - \frac{1}{\rho_l} \right) \frac{(T + 273.15)g}{h_{vl}} \frac{\frac{k_{rv} \rho_v^2}{\mu_v} + \frac{k_{rl} \rho_l^2}{\mu_l}}{\frac{k_{rv} \rho_v}{\mu_v} + \frac{k_{rl} \rho_l}{\mu_l}} \quad (3)$$

Here K is thermal conductivity, T is temperature in °C, k is absolute permeability, ρ is density, $h_{vl} = h_v - h_l$ is vaporization enthalpy, g is acceleration of gravity, μ is viscosity, k_r is relative permeability, and subscripts l and v denote liquid and vapor phases, respectively.

From Eq. (2) it can be seen that the heat flux associated with balanced liquid-vapor counterflow will tend to zero as temperatures approach the critical point (374.15 °C for pure water). It is well known that for a given convective heat flux a balanced liquid-vapor counterflow is possible in two distinct conditions, corresponding to vapor-dominated and liquid-dominated heat pipes, respectively (Martin et al., 1976; Pruess, 1985). Formally, this can be seen from Eq. (2), which for given Q_{conv} has one solution in which k_{rl} is small and another in which k_{rv} is small. In the vapor-dominated state the vertical pressure gradient is somewhat larger than vapor-static, so that there is a large effective force for downward flow of liquid. A balanced counterflow of vapor and liquid is then possible for conditions of very small liquid relative permeability (large vapor saturation). Conversely, in the liquid-dominated state there is a large force for upward vapor flow, and under conditions of balanced counterflow both vapor saturation and vapor relative permeability are small.

We have evaluated Eqs. (1) - (3) over a wide range of temperatures, assuming that the sum of liquid and vapor relative permeabilities is equal to 1, as is appropriate for a fractured medium (Pruess et al., 1983). Temperature and pressure dependence of water properties was computed from equations given by the International Formulation Committee (1967). The results are plotted in Figures 2 and 3. It is seen that vapor-dominated heat pipes show only modest variations in heat transfer rates over the temperature range from 150 to 300 °C. In contrast, heat flux in liquid-dominated heat pipes has

a fairly sharp maximum near 320 °C. However, no dramatic reduction in heat flux is observed for temperatures up to 350 °C in either case.

As an alternative to Eqs. (1) - (3) one can write

$$kk_{rv} = \frac{Q - K \frac{dT}{dz}}{\mu_v \left[\frac{h_{vl}}{\left(\frac{1}{\rho_v} - \frac{1}{\rho_l} \right) (T + 273.15)} \frac{dT}{dz} - \rho_v g \right]} \quad (4)$$

which expresses effective vapor permeability $k \cdot k_{rv}$ as a function of total heat flux, reservoir temperature, and temperature gradient. (Note that all water properties appearing in Eq. (4) are to be evaluated on the saturation line; i.e., they are functions of temperature only.) An analogous relationship can be written for effective liquid permeability. For a vapor-dominated reservoir total heat flux is known from the conductive gradient in the caprock. With Eq. (4) it should then be possible to obtain estimates of vertical permeability for vapor and liquid from data on temperatures and temperature gradients. If for relative permeabilities in a fractured system one further assumes that $k_{rv} + k_{rl} = 1$ one could obtain absolute vertical permeability k at each depth level, and also liquid and vapor relative permeabilities separately. In practice, estimation of vertical permeability from Eq. (4) is problematic, even if good data on undisturbed formation temperatures are available. We have performed numerical simulations of heat pipes of varying vertical permeability, and have analyzed the simulated temperature data by means of Eq. (4) and an analogous relationship for effective liquid permeability. In a liquid-dominated heat pipe vertical pressure gradient deviates little from hydrostatic, so that small inaccuracies in temperatures translate into large variations for estimated permeabilities. In vapor-dominated heat pipes the deviations from a vapor-static gradient tend to be much larger, so that practically useful permeability estimates may be possible.

It is instructive to apply Eq. (4) to some of the temperature data from Larderello, even though the assumptions on which it is based are not valid in a producing reservoir, where there is a large net upward flow. Figure 4 shows results for vertical permeability obtained from well A temperatures, which are particularly interesting because the transition to a higher temperature gradient is well defined near 2400 m depth (see Fig. 1). The permeability values obtained represent lower limits, because the analysis did not take into account that vertical vapor fluxes are substantially increased in response to exploitation. An alternative estimation of vertical permeability near well A can be obtained by assuming that vertical vapor flux is equal to the stabilized long-term production rate

at Larderello. This will provide an upper limit for vertical permeability, because vertical flux will in fact diminish with depth as fluid is being released from storage. Furthermore, at shallower horizons the reservoir has evolved single-phase vapor conditions with smaller pressures and larger pressure gradients than obtained from the assumption that pressures are equal to saturation pressures at given temperatures. Calculating permeability from a given vapor flux and a low estimate for pressure gradient will result in an upper limit for permeability. Assuming a representative value of 100 tonnes/hour/km² for stabilized production rate at Larderello results in estimates of vertical permeability approximately 40 times larger than obtained from the assumption of undisturbed natural conditions (see Fig. 4). Actual vertical permeability should be intermediate between the two estimates, being closer to the values inferred from the stabilized production flux at shallower horizons, and trending more towards the values obtained from the natural state flow model at greater depth, where conditions are less severely affected by exploitation.

NUMERICAL SIMULATIONS

A more precise estimation of vertical permeability should be possible from numerical simulations. A numerical model for long-term field depletion must be consistent with the concepts of heat transfer outlined in the previous section, and it must adequately represent observed trends of production rates and flowing enthalpies, as well as reservoir pressures. The main constraints on a model are (1) the total vertical heat flux in the natural state, which is rather well known from the depth to reservoir top and the undisturbed temperature there [from well A data we have $Q = K \cdot dT/dz = 2.3 \times 0.49 = 1.12 \text{ W/m}^2$]; (2) a rather rapid initial decline in flow rate of most wells by a factor of typically 3-5 in the first few years of production, followed by a stabilization of rates; (3) a long-term rise in produced enthalpy, from initial values near 2800 kJ/kg to values near 2900 kJ/kg and larger; and (4) a trend of increasing temperatures of produced fluids over some 20 years of exploitation, at a rate of 1 - 1.5 °C/year (Sestini, 1970); presently temperatures at the reservoir top are near 240 °C.

Using LBL's geothermal reservoir simulator MULKOM (Pruess, 1983), we have performed numerical simulations of one-dimensional vertical sections which were designed to represent the important attributes of the Larderello system in a generic way. Vertical permeability structure was chosen based on the results of the analysis presented above (see Fig. 4). Initial conditions are not known but can be reasonably well constrained from available temperature data and the heat pipe mechanism of vertical heat transfer. In Figure 5 we have plotted a temperature profile corresponding to a

vapor-static pressure gradient, with $T = 240^{\circ}\text{C}$ at 500 m depth. Temperatures increase with depth by approximately 4°C per km. In realistic vapor-dominated heat pipe conditions temperature and pressure gradients may be 1.5 - 5 times larger (depending on heat flux and vertical permeability), but it is clear that a vapor-dominated heat pipe can not reach temperatures of 300°C or more at 3000 m depth as have been measured in the field. Clearly, therefore, at some depth a transition to a liquid-dominated heat pipe must have been present in the natural state. The depth at which this transition occurred is unknown; it was chosen as 2100 m in the simulations. This appears reasonable in view of measured temperatures, and the inferred reduction in vertical permeability near 2100 m depth (see Fig. 4). Ultimately, of course, this as well as other modeling assumptions and parameters need to be verified by comparison of simulated reservoir behavior with field data.

Table 1 lists parameters used in the simulations, which are intended to represent typical conditions at Larderello; the large irreducible liquid saturation (80%) was chosen to approximately account for the large enthalpies of fluids produced from fractured-porous media. Selected results for production rates per km^2 , production enthalpies, and temperatures at reservoir top (at 500 m depth) are given in Figures 6 and 7. Before discussing these results we will briefly give a qualitative discussion of simulated reservoir response to exploitation.

In response to fluid withdrawal boiling will be induced in the reservoir, with accompanying increase in vapor saturation and decline of reservoir pressure and temperature. These effects will be initially confined to the vicinity of the production interval (reservoir top), but will over time propagate to greater reservoir depths. Important effects are induced when the disturbance in reservoir conditions reaches the liquid-dominated heat pipe at depth. In this region large vertical pressure gradients are present, and a strong increase in the rate of vapor upflow will occur when vapor saturation and mobility increase. The upflowing vapor will in part condense at shallower levels, as a consequence of which temperature decline may slow down or even reverse in the condensation zone.

In a porous medium model it is possible to adequately represent the long-term trend of production rate, but produced enthalpies and temperatures at the reservoir top are underpredicted (see Fig. 6). We made various modifications to parameters (see Table 1) in order to enhance rate and enthalpy of fluids rising from depth, including: increase in vertical permeability all the way to the upper limit obtained above (see Fig. 4); decrease in reservoir porosity; downward extension of the permeable reservoir to a depth of 4300 m, where

temperatures in the liquid-dominated heat pipe reach 355.6°C . These modifications were tried one at a time as well as in combination, but they were unable to deliver enthalpies as large as observed in the field. Simulated flowing enthalpies reached maximum levels of 2830 kJ/kg.

In order to obtain higher-enthalpy fluids two possible mechanisms can be considered. One possibility is that supercritical fluids of very high enthalpy may flow up from great depth and make increasing contributions to production as shallower horizons are being depleted. Such fluids have been encountered in the deep drilling at Larderello (Cappetti et al., 1985). An alternative possibility is that fluids of very high enthalpy may be obtained from a process of enthalpy enhancement which is peculiar to two-phase flow in fractured-porous media. When low-permeability rocks containing two-phase fluid are made to discharge into fractures, the flowing enthalpy of the discharge can be substantially enhanced by an interplay between two-phase flow and heat conduction in the rock matrix (Pruess and Narasimhan, 1982).

Contributions of supercritical fluids are very difficult to evaluate. In the present work we have focussed on fracture effects for subcritical two-phase fluids. Several simulation runs were made in which fracture-matrix interactions were represented using a multiple interacting continua approach (MINC; Pruess and Narasimhan, 1982, 1985). Results given in Figure 6 indicate that substantially higher flowing enthalpies (up to 2875 kJ/kg) and higher temperatures at the reservoir top were obtained. Figure 7 shows that there is a complex structure to reservoir depletion at different depths, with important flow effects occurring in the vicinity of the original transition from vapor- to liquid-dominated conditions (2100 m depth). The depletion mechanism is rather different for fractured than for porous systems. The former permit far better access to heat stored in deep reservoir rocks. We expect that a satisfactory agreement between the predictions from a fractured reservoir model and field observations will be obtainable through a more extensive parameter search.

The observed long-term rise in produced fluid temperatures has not yet been modeled. We believe that this effect arises from localized boiling after a well is first opened, which causes a rapid initial temperature drop to near 210°C ; followed by reheating of the formations by high-enthalpy fluids from depth. Modeling of these processes is in progress; it requires a rather detailed spatial resolution near the well feeds, especially for horizontal flow.

CONCLUSIONS

We have presented a preliminary analysis of permeability structure and fluid and heat flow conditions in the deeper horizons of the Larderello geothermal system. Our main observations and findings are:

- (1) Measurements in deep Larderello wells have indicated formation temperatures near 300 °C at 3000 m depth, and even higher temperatures at greater depth.
- (2) From an analysis of heat transfer mechanisms we suggest that a transition from vapor-dominated to liquid-dominated conditions must have been present in the natural state of the Larderello geothermal system. No reliable determination of the depth at which this transition occurred has yet been made, but a depth of approximately 2000 m or more appears most likely.
- (3) From temperature-depth data in two-phase reservoirs it is in principle possible to estimate vertical permeability.
- (4) For exploited reservoirs such as Larderello, reconstruction of permeability and temperature trends with depth can be made indirectly, using numerical simulation. Our preliminary results indicate that production of high-enthalpy fluids can be explained from two-phase flow effects in a fractured-porous medium.

ACKNOWLEDGEMENT

The U.S. Department of Energy, Geothermal Technology Division, provided financial support to LBL for its participation in this study under Contract No. DE-AC03-76SF00098. A critical review of the paper by M. Lippmann and S. Benson is appreciated. For assistance in the preparation of the manuscript the authors are indebted to L. Fairbanks and D. Swantek.

REFERENCES

- Barelli, A. and Palama, A., A New Method for Evaluating Formation Equilibrium Temperature in Holes During Drilling, *Geothermics*, Vol. 10, No. 2, pp. 95-102, 1981.
- Cappetti, G., Celati, R., Cigni, V., Squarci, P., Stefani, G., and Taffi, L., Development of Deep Exploration in the Geothermal Areas of Tuscany, Italy, 1985 International Symposium on Geothermal Energy, International Volume, *Geothermal Resources Council*, pp. 303-309, 1985.
- D'Amore, F., and Truesdell, A. H., Models for Steam Chemistry at Larderello and The Geysers, Proceedings Fifth Workshop Geothermal Reservoir Engineering, Stanford, California, pp. 283-297, 1979.
- Drenick, A., Pressure-Temperature-Spinner Survey in a Well at The Geysers, paper presented at 11th Workshop Geothermal Reservoir Engineering, Stanford University, Stanford, California, January 1986.
- Ferrara, G., Panichi, C., Stefani, G., Remarks on the Geothermal Phenomenon in an Extensively Exploited Field, Results of an Experimental Well, *Geothermics, Special Issue 2*, Vol. 2, Part 1, pp. 578-586, 1970.
- Grant, M. A., Donaldson, I. G., and Bixley, P. F., *Geothermal Reservoir Engineering*, Academic Press, New York, 1982.
- International Formulation Committee, A Formulation of the Thermodynamic Properties of Ordinary Water Substance, IFC Secretariat, Düsseldorf, Germany, 1967.
- Martin, J. C., Wegner, R. E., and Kelsey, F. J., One-Dimensional Convective and Conductive Geothermal Heat Flow, Proceedings, Second Workshop on Geothermal Reservoir Engineering, Stanford University, pp. 251-262, 1976.
- Pruess, K., Development of the General Purpose Simulator MULKOM, Annual Report 1982, Earth Sciences Division, report LBL-15500, Lawrence Berkeley Laboratory, 1983.
- Pruess, K., A Quantitative Model of Vapor-Dominated Geothermal Reservoirs as Heat Pipes in Fractured Porous Rock, Transactions, Geothermal Resources Council, Vol. 9, Part II, pp. 353-361, 1985.
- Pruess, K., Bodvarsson, G. S., and Stefansson, V., Analysis of Production Data from the Krafla Geothermal Field, Iceland, paper presented at Ninth Workshop on Geothermal Reservoir Engineering, Stanford University, Stanford, CA., December 1983.
- Pruess, K., and Narasimhan, T. N., On Fluid Reserves and the Production of Superheated Steam from Fractured, Vapor-Dominated Geothermal Reservoirs, *Journal of Geophysical Research*, Vol. 87, No. B11, pp. 9329-9339, 1982.
- Pruess, K., and Narasimhan, T. N., A Practical Method for Modeling Fluid and Heat Flow

in Fractured Porous Media, *Society of Petroleum Engineers Journal*, Vol. 25, No. 1, pp. 14-26, February 1985.

Sestini, G., Superheating of Geothermal Steam, *Geothermics*, Special Issue 2, pp. 622-648, 1970.

Straus, J. M., and Schubert, G., One-Dimensional Model of Vapor-Dominated Geothermal Systems, *Journal of Geophysical Research* Vol. 86, No. B10, pp. 9433-9438, October 1981.

Truesdell, A. H., and White, D. E., Production of Superheated Steam from Vapor-Dominated

Geothermal Reservoirs, *Geothermics*, Vol. 2, No. 3-4, pp. 154-173, September-December, 1973.

Weres, O., Tsao, K., and Wood, B., Resource, Technology and Environment at The Geysers, Lawrence Berkeley Laboratory report LBL-5231, Berkeley, California, July 1977.

White, D. E., Muffler, L. J. P., and Truesdell, A. H., Vapor-Dominated Hydrothermal Systems Compared with Hot-Water Systems, *Economic Geology*, Vol. 66, No. 1, pp. 75-97, 1971.

Table 1. Parameters for Numerical Simulations*

Parameter	Value
Formation Parameters	
rock grain density	2600 kg/m ³
rock specific heat	920 J/kg . °C
formation heat conductivity	2.3 W/m . °C (caprock) 2.7 - 3.5 W/m . °C (reservoir)
formation porosity	3 - 5%
vertical permeability ‡	0.1 - 24 x 10 ⁻¹⁵ m ²
effective fracture porosity †	0.1 - 0.5%
rock matrix permeability †	0.1 - 2.0 x 10 ⁻¹⁸ m ²
fracture spacing †	50 m
depth of permeable reservoir	3200 - 4300 m
liquid relative permeability	$k_{rl} = (S_l - 0.8)/0.2$
vapor relative permeability	$k_{rv} = 1 - k_{rl}$
capillary pressure	0
Initial Conditions	
temperatures**	240 °C at 500 m depth; beneath 500 m heat pipe with a heat flux of 1.12 W/m ² ; vapor-dominated down to 2100 m depth, then liquid-dominated
pressures	saturation pressures at prevailing temperatures
liquid saturation	as obtained for steady-state heat pipe with heat flux of 1.12 W/m ² (slightly larger than 80% in vapor-dominated section; close to 100 % in liquid-dominated section)
Production Specifications ("Wells")	
flowing bottomhole pressure	5 bars
productivity index #	4.88 x 10 ⁻¹⁷ m ³

* parameters for which a range is given were varied in the simulations;

‡ variation with depth shown in Figure 4;

† for fractured medium simulations only;

** see Figure 7;

adjusted to obtain an early-time rate approximately four times larger than stabilized rate of 100 tonnes/hour/km²

Table 2. Specifications of Cases shown in Figures 6 and 7†.		
	Case A	Case B
reservoir description	porous medium	fractured-porous
vertical permeability	low*	high*
matrix porosity	5%	5%
matrix permeability	*	$0.2 \times 10^{-18} \text{ m}^2$
fracture porosity	(no fractures)	0.1%
depth to bottom of permeable reservoir	3200 m	3200 m

† additional specifications as in Table 1.

*see Figure 4

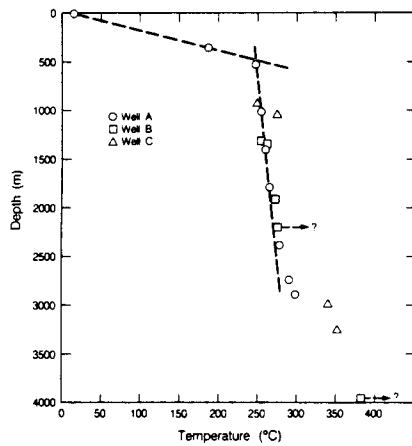


Figure 1. Measured temperatures for three deep wells in the central area of Larderello. The lines are drawn to guide the eye.

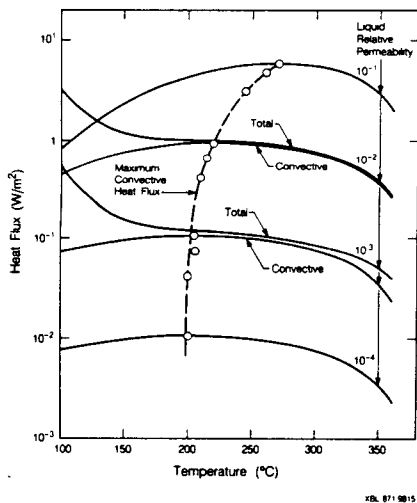


Figure 2. Heat flux for balanced steam-water counterflow in vapor-dominated conditions (permeability 10^{-15} m^2 ; formation heat conductivity $2.5 \text{ W/m} \cdot ^\circ\text{C}$).

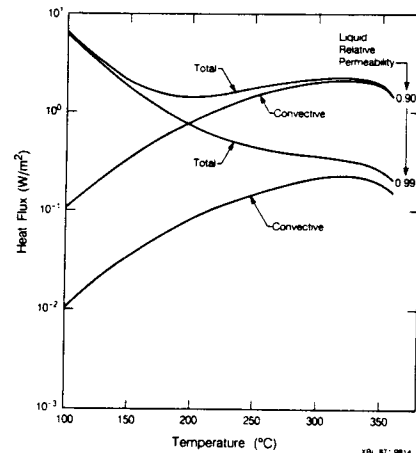


Figure 3. Heat flux for balanced steam-water counterflow in liquid-dominated conditions (permeability 10^{-15} m^2 ; formation heat conductivity $2.5 \text{ W/m} \cdot ^\circ\text{C}$).

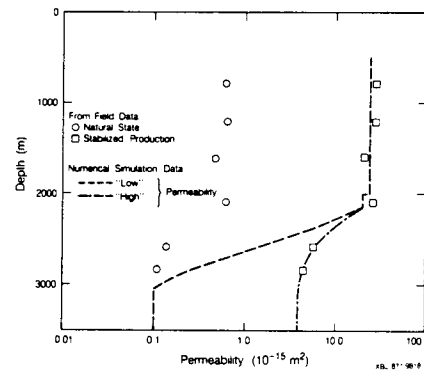


Figure 4. Vertical permeability distributions as derived from temperature data for well A. Permeability values used in numerical simulations are also shown.

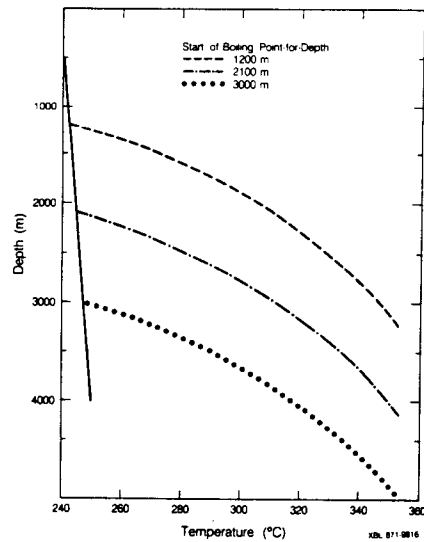


Figure 5. Temperature versus depth for boiling point-for-depth conditions beneath a vapor-static gradient.

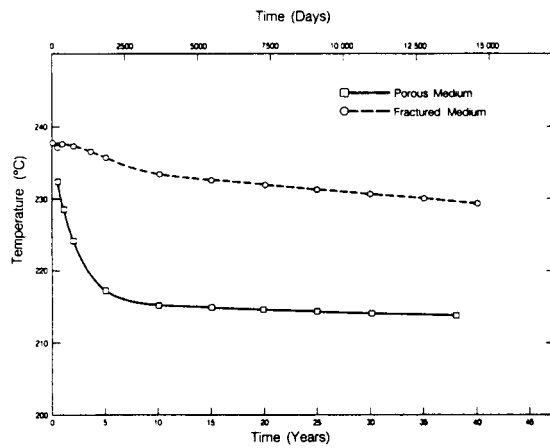
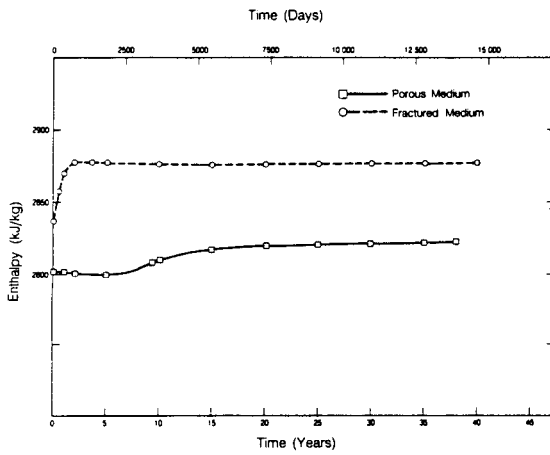
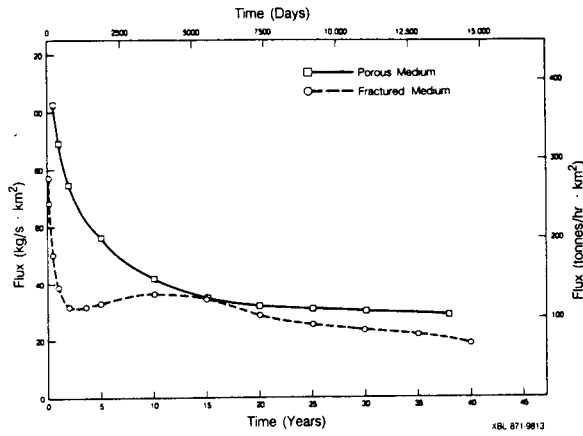


Figure 6. Simulated results for flow rates, enthalpies, and temperatures of produced fluids. Parameters are defined in Tables 1 and 2.

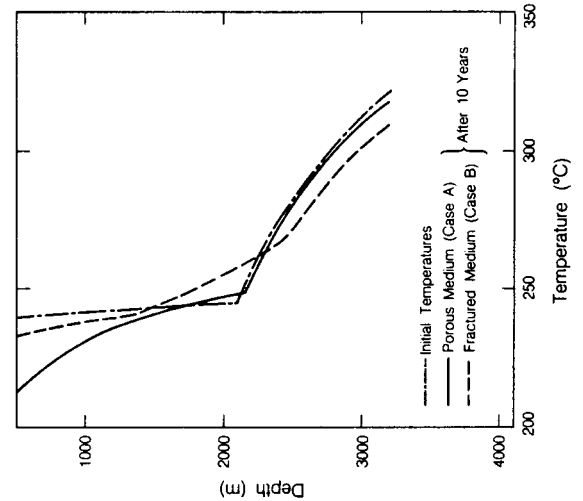
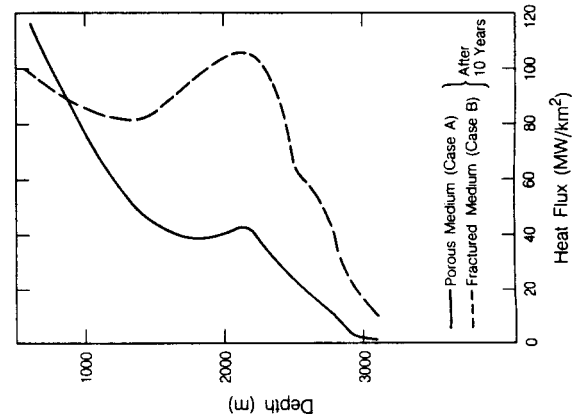
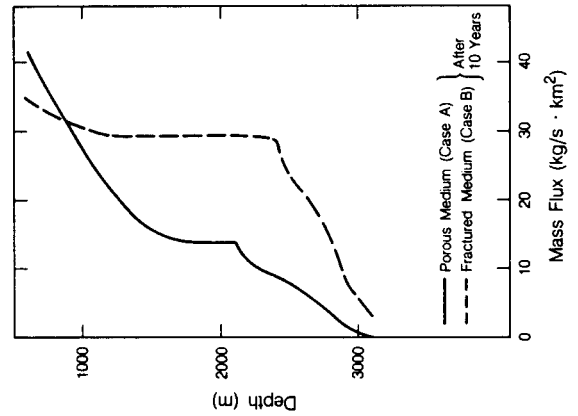


Figure 7. Simulated temperature profiles, and heat and fluid flow rates, after 10 years of production. Parameters are defined in Tables 1 and 2. The initial temperature profile corresponding to a steady state heat pipe with a flux of 1.12 MW/km^2 is also shown.